J|A|C|S
ARTICLES
Published on Web 01/12/2006

# Characterizing Challenging Microcrystalline Solids with Solid-State NMR Shift Tensor and Synchrotron X-ray Powder Diffraction Data: Structural Analysis of Ambuic Acid

James K. Harper,[†] David M. Grant,*[,†] Yuegang Zhang,[‡] Peter L. Lee,[‡] and Robert Von Dreele[‡]

*Contribution from the Department of Chemistry, University of Utah, 315 South 1400 East, Salt Lake City, Utah 84112, and Argonne National Laboratory, Advanced Photon Source, Argonne, Illinois 60439*

Received August 15, 2005; E-mail: grant@chemistry.utah.edu

***Abstract:*** Synchrotron X-ray powder diffraction and solid-state $^{13}C$ NMR shift tensor data are combined to provide a unique path to structure in microcrystalline organic solids. Analysis is demonstrated on ambuic acid powder, a widely occurring natural product, to provide the complete crystal structure. The NMR data verify phase purity, specify one molecule per asymmetric unit, and provide an initial structural model including relative stereochemistry and molecular conformation. A refinement of X-ray data from the initial model establishes that ambuic acid crystallizes in the $P2_1$ space group with unit cell parameters $a = 15.5047(7)$, $b = 4.3904(2)$, and $c = 14.1933(4)$ Å and $\beta = 110.3134(3)°$. This combined analysis yields structural improvements at two dihedral angles over prior NMR predictions with differences of 103° and 37° found. Only minor differences of ±5.5°, on average, are observed at all remaining dihedral angles. Predicted hydroxyl hydrogen-bonding orientations also fit NMR predictions within ±6.9°. This refinement corrects chemical shift assignments at two carbons and reduces the NMR error by ~16%. This work demonstrates that the combination of long-range order information from synchrotron powder diffraction data together with the accurate shorter range structure given by solid-state NMR measurements is a powerful tool for studying challenging organic solids.

## Introduction

Structural characterizations of many materials are difficult due to their insolubility, reluctance to form crystals suitable for single crystal X-ray diffraction, or lack of suitably positioned hydrogens necessary for accurate solution NMR analysis. Solid-state NMR (SSNMR) can enhance structural analysis in these cases. Recently, SSNMR methods have demonstrated the capability of providing complete de novo structures for entire molecules.[1] These methods establish structure through the measurement of properties such as dipolar interactions,[1a,d] spin diffusion,[1b] and chemical shift tensors.[1c] Measurements are usually performed at numerous sites throughout the molecule to reduce ambiguity. Isotopic labeling ($^{13}C$ and $^{15}N$) is typically required, but the structure[1c] for a product at natural abundance has also recently appeared, providing the opportunity to investigate molecules that are difficult to label. Most of the reported SSNMR methods presently have some ambiguities in the predicted structures, and, more significantly, they provide only modest information on long-range lattice order. While considerable effort has been directed toward minimizing uncertainties,[1,2] inclusion of an independent approach is needed to provide lattice detail, verify structural conclusions, and allow for further refinement of coordinates. X-ray powder diffraction (XRPD) provides such a method.

Structural determination by XRPD is becoming increasingly routine due to advances in structure solving algorithms and software as well as the development of synchrotron powder diffraction techniques.[3,4] Synchrotron data provide both the high resolution and the increased signal-to-noise ratio needed for accurate long-range structural analysis.[5] Additionally, shorter total exposure times of tens of seconds reduce radiation damage to organic samples. An image plate detector with Debye−Scherrer geometry can also reduce problems with preferred orientations.[6] However, indexing of powder patterns remains difficult when there is overlap of Bragg peaks or contamination

[†] University of Utah.
[‡] Argonne National Laboratory.

(1) (a) Rienstra, C. M.; Tucker-Kellogg, L.; Jaroniec, C. P.; Hohwy, M.; Reif, M. T.; McMahon, B. T.; Lozano-Pérez, T.; Griffin, R. G. *Proc. Natl. Acad. Sci. U.S.A.* **2002**, *99*, 10260. (b) Castellani, F.; van Rossum, B.-J.; Diehl, A.; Schubert, M.; Oschkinat, H. *Nature* **2002**, *420*, 98. (c) Harper, J. K.; Barich, D. H.; Hu, J.-Z.; Strobel, G. A.; Grant, D. M. *J. Org. Chem.* **2003**, *68*, 4609. (d) Jaroni, C. P.; MacPhee, C. E.; Bajaj, V. S.; McMahon, M. T.; Dobson, C. M.; Griffin, R. G. *Proc. Natl. Acad. Sci. U.S.A.* **2003**, *101*, 711.
(2) Kim, S.; Quine, J. R.; Cross, T. A. *J. Am. Chem. Soc.* **2001**, *123*, 7292.
(3) Harris, K. D. M.; Tremayne, M. *Chem. Mater.* **1996**, *8*, 2554.
(4) (a) Structure determination from powder diffraction data (*International Union of Crystallography, Monographs on Crystallography No. 13*; David, W. I. F., Shankland, K., McCusker, L. M., Baerlocher, C., Eds.; Oxford University Press: New York, 2002). (b) Crystal structure determination from powder diffraction data (*Transactions of the American Crystallographic Association*; Clearfield, A., Ed.; American Crystallographic Association: Buffalo, New York, 2002; Vol. 37).
(5) Lang, J. C.; Srajer, G.; Wang, J.; Lee, P. L. *Rev. Sci. Instrum.* **1999**, *70*, 4457.
(6) Howard, C. J.; Kisi, E. H. *J. Appl. Crystallogr.* **2000**, *33*, 1434.

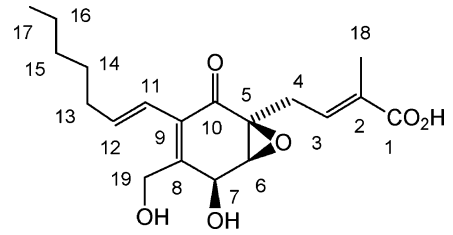


***Figure 1.*** Structure of ambuic acid.

from minor polymorphs or other materials. Typical organic samples containing only C, O, N, and H are also problematic because weak diffractions are observed. These problems are particularly evident in structures having large unit cell dimensions. These challenges are somewhat alleviated when independent information such as SSNMR data are available.

SSNMR provides structural information vital to accurate XRPD analysis including phase and chemical purity, the number of molecules per asymmetric unit ($Z'$), the presence of molecular motion, and reasonable starting structures. Moreover, because NMR is nondestructive, the same sample can be used in XRPD analysis to remove the possibility of introducing a second polymorph. Incorporation of these independent data accelerates the indexing process and reduces the number of trials needed to confirm the space group. Likewise, the risk of falling into false minima by regression methods is decreased.

X-ray powder data have previously been combined with SSNMR data to examine structure in cimetidine,[7] *N*-(*p*-tolyl)-dodecylsulfonamide,[8] and theophylline.[9] In these studies, SSNMR measurements of isotropic shifts or dipolar interactions have been included to constrain the XRPD refinement. A potentially more sensitive alternative is the inclusion of the three principal values per nuclear position found in the NMR shift tensor. These values are more sensitive to structure than isotropic shifts, in general. Additionally, natural abundance samples can usually be used, avoiding the need for isotopic labeling as required for measurement of intramolecular distances from dipolar interactions. Preliminary investigation in combining shift tensor and XRPD data has recently provided a partial structure for a novel polymorph of taxol.[10]

Herein, we described the complete crystal structure for ambuic acid (Figure 1) using a combination of synchrotron XRPD and $^{13}$C SSNMR tensor data.[11] Ambuic acid is an antifungal agent first isolated from a quiescent fungus (*Pestalotiopsis microspora*) found in an orchid collected in Papua New Guinea.[12] Subsequent work demonstrated that ambuic acid is far more abundant than originally appreciated. Indeed, plant tissue samples obtained from the rainforests of several continents have been found to contain *Pestalotiopsis* and *Monochaetia* spp., both of which produce ambuic acid.[12] Because fungi belonging to the *Pestalotiopsis* genus are among the most frequently isolated microbes in plant tissue, ambuic acid is likely to be one of the more widely occurring natural products. The refinement described here provides structural details such as hydrogen-bonding interactions that may be relevant to biological activity.

The XRPD/SSNMR analyses provide lattice structure and refined coordinates and verify that most features of the SSNMR structure predicted earlier are correct. These data also illustrate how the combination of methods eliminates errors arising from a single type of data. Modest errors, observed in the prior NMR structure of ambuic acid, consist of conformational errors at two bonds (i.e., rotation about C4−C5 and C12−C13) and chemical shift misassignments at two carbons (C13 and C14). Likewise, the structure predicted solely from XRPD data contains minor errors that are strongly reflected in computed NMR tensors. Procedures for identifying and treating these errors in future studies are outlined.

## Experimental Section

Synchrotron XRPD data were collected using the 1-BM beam line at the Advanced Photon Source (Argonne National Laboratory). Analysis used Debye−Scherrer geometry with a Mar345 image plate detector and a wavelength of 0.619333 Å. The wavelength was calibrated using a NIST 640c silicon standard powder with a Si (111) crystal analyzer and a scintillation counter point detector. The sample-to-detector distance of 453.443 mm and detector tilt angles were calibrated using a NIST 660a $LaB_6$ standard. Data were collected at room temperature using an ambuic acid powder sample loaded into a 0.8 mm capillary spun at 2 Hz. Five diffraction frames were collected in 20 s exposures and summed. Diffraction frames were also collected with an empty capillary and subtracted from the data frames. The powder pattern was integrated with a 30° azimuthal angle of the image plate data and the Fit2d program.[13] The pattern was indexed with the Dicvol program,[14] and the structure was solved with DASH[15] and PSSP[16] using direct space methods and employing the SSNMR structure[1c] as the initial model, with molecular translation, rotation, and all flexible intramolecular torsion angles varied. It was found necessary to vary all torsion angles over a 360° range as refinement using the rigid SSNMR model gave XRPD errors that indicated the need for additional conformational adjustment. Rietveld refinement was performed using the GSAS program[17] with restraints on bond distances and valence angles taken from ab initio computations. Isotropic thermal parameters for each non-hydrogen atom were refined individually. For carbon atoms 14−17, these values were observed to be significantly larger than at other atoms. A difference Fourier map ($F_o - F_c$) made without the C14−C17 fragment in the model showed disorder at these positions. In the final refinement, the thermal parameters for C14−C17 were thus refined individually, while all other non-hydrogen atoms were constrained to be identical. In the final refinement, hydrogen atom positions were fixed to those determined in the ab initio computations. The accuracy of hydrogen positions was verified by the high-quality fit to SSNMR data that are particularly sensitive to proton positions.[18]

Ambuic acid sample isolation[12] and the solid-state NMR/computational analyses providing initial structure have been described elsewhere.[1c] All NMR tensors were computed using Gaussian 03,[19] the B3PW91 method,[20] and the D95** basis set. Most structural refinements were

(7) Middleton, D. A.; Peng, X.; Saunders, D.; Shankland, K.; David, W. I. F.; Markvardsen, A. *J. Chem. Commun.* **2002**, 1976.
(8) Rajeswaran, M.; Blanton, T. N.; Zumbulyadis, N.; Giesen, D. J.; Conesa-Moratilla, C.; Misture, S. T.; Stephens, P. W.; Huq, A. *J. Am. Chem. Soc.* **2002**, *124*, 14450.
(9) Smith, E. D. L.; Hammond, R. B.; Jones, M. J.; Roberts, K. J.; Mitchell, J. B. O.; Price, S. L.; Harris, R. K.; Apperley, D. C.; Cherryman, J. C.; Docherty, R. *J. Chem. Phys. B* **2001**, *105*, 5818.
(10) Harper, J. K.; et al. *Cryst. Growth Des.* **2005**, *5*, 1737.
(11) A preliminary report of this work was given by: Zhang, Y. *The Pharmaceutical Powder X-ray Diffraction Symposium*; 23−25, February 2004, Hilton Head, SC.
(12) (a) Li, J. Y.; Harper, J. K.; Grant, D. M.; Tombe, B. O.; Bashyal, B.; Hess, W. M.; Strobel, G. A. *Phytochemistry* **2001**, *56*, 463. (b) Daisy, B.; Strobel, G. *Microbiol. Mol. Biol. Rev.* **2003**, *67*, 491.
(13) Hammersley, A. P. ESRF Internal Report, EXP/AH/95-01, 1995, FIT2D V5.18 Reference Manual V1.6.
(14) Boultif, A.; Louër, D. *J. Appl. Crystallogr.* **1991**, *24*, 987.
(15) David, W. I. F.; Shankland, K.; Shankland, N. *Chem. Commun.* **1998**, 931.
(16) Pagola, S.; Stephens, P. W. *Mater. Sci. Forum* **2000**, *321−324*, 40.
(17) Larson, A. C.; Von Dreele, R. B. *GSAS − General Structure Analysis System*; Los Alamos Laboratory Report, LA-UR-86-748, 1987.
(18) Fang, L.; Phung, C. G.; Alderman, D. W.; Grant, D. M. *J. Am. Chem. Soc.* **1996**, *118*, 10629.
(19) Frisch, M. J.; et al. *Gaussian 03*, revision A.9; Gaussian, Inc.: Pittsburgh, PA, 2003.

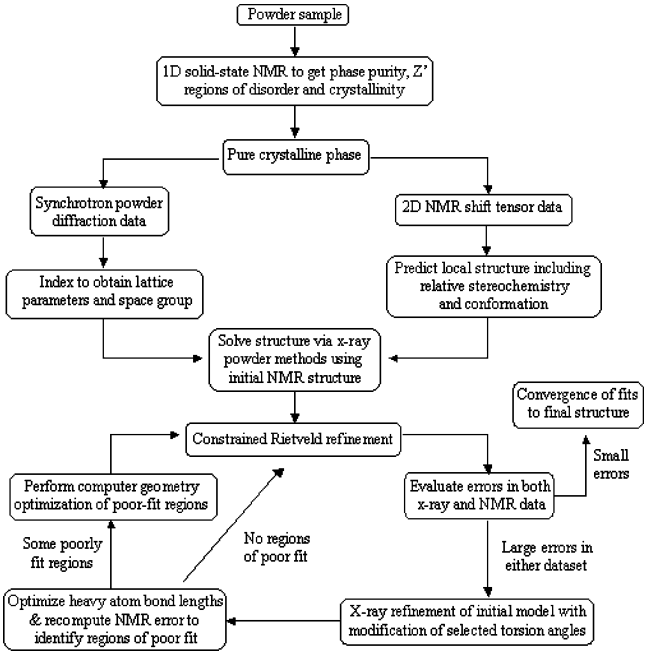


***Figure 2.*** An algorithm for combining X-ray and solid-state NMR data. Poor fits to data are defined here as NMR errors greater than 10 ppm in any single principal value and X-ray weighted Rietveld parameters larger than 10%.

performed using Gaussian 03 at the B3LYP/D95* level of theory.[20a,21] However, refinement of OH hydrogens required inclusion of a number of atoms from neighboring molecules. A semiempirical optimization (AM1[22]) was therefore employed to avoid the prohibitive computation time associated with ab initio or density functional methods (DFT) for such a large system.

## Results and Discussion

**Structural Insights from Solid-State NMR Data.** Ambuic acid was selected for this initial investigation because it has proven challenging to analyze by traditional methods.[12] Single crystal X-ray diffraction is not available due to the difficulty of obtaining high-quality single crystals. Likewise, solution NMR is ambiguous regarding structural details, such as stereochemistry, due to the absence of suitably positioned hydrogens at key positions as discussed elsewhere.[12]

Despite these difficulties, a novel approach involving SSNMR and computational methods provided a high probability structure.[1c] These analyses provided coordinates for the most probable structure, denoted here as **I**,[1c] and assign structural features including relative stereochemistry, conformation about five bonds (i.e. C4−C5, C7−O, C19−O, C9−C11, and C8−C19), and hydrogen-bonding arrangements at three positions including an intermolecular hydrogen bond between carboxyl groups. The prediction of the carboxyl hydrogen bonding is particularly relevant to crystallographic studies as a survey of packing modes in monocarboxylic acids has demonstrated that that COOH moieties almost invariably interlink as cyclic dimers or catameric chains bonded along a $2_1$ axis.[23] Thus, the lattice contains either a 2-fold or a $2_1$-screw axis involving the COOH moiety. The

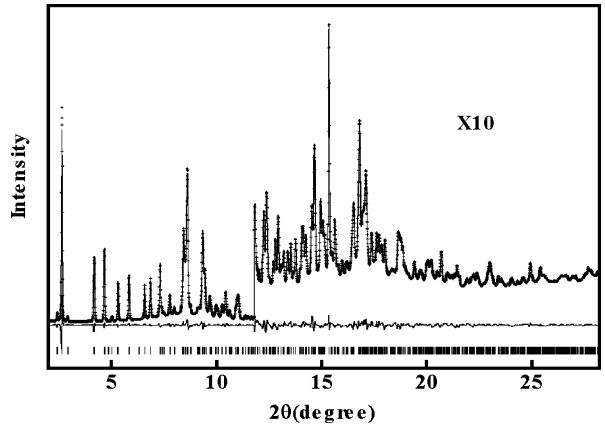


***Figure 3.*** Restrained Rietveld fitting of the ambuic acid powder diffraction data. Crosses denote observed data with the overlaid line representing the computed profile. The difference between observed and calculated data is included at the bottom of the plot. Peak positions are indicated by tick marks below the corresponding peaks.

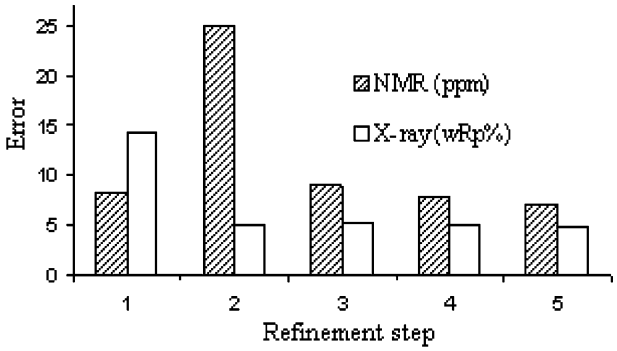


***Figure 4.*** A plot of error versus structural refinement step showing fits to both SSNMR and XRPD data. Steps 1 and 2 show that refinements involving only NMR or XRPD data, respectively, leave errors that are easily identified by the alternative analysis technique. Step 3 includes both data types and combines Rietveld refined dihedral angles with ab initio calculated bond lengths and valence angles. Steps 4 and 5 involve minor structural modifications and illustrate how the error analysis can guide even marginal structural refinements. The SSNMR and XRPD techniques derive error estimates differently, hence the absolute magnitude of the errors for the two techniques cannot be directly compared for a given step, but show the general improvements in the refinement.

SSNMR data also specify a structure with $Z' = 1$ and demonstrate that the solid is a single phase. However, these data still provide an incomplete view of long-range lattice order that XRPD data can potentially provide.

**Establishing Lattice Detail with X-ray Powder Diffraction Data.** X-ray powder data for ambuic acid were acquired using the sample previously analyzed by SSNMR[1c] to eliminate uncertainty regarding sample preparation. Possible space groups were constrained to $P2$ and $P2_1$ based on the knowledge that ambuic acid is chiral and consists of a single enantiomer,[24] the SSNMR observation of $Z' = 1$, and reasonable calculated densities. The high resolution of the synchrotron data allowed for indexing of the powder pattern and gave a monoclinic cell with parameters $a = 15.5047(7)$ Å, $b = 4.3904(2)$ Å, and $c = 14.1933(4)$ Å, $\beta = 110.3134(3)°$, and volume $= 907.08$ Å$^3$. The space group was identified as $P2_1$, and the structure was solved as described in the Experimental Section (wRp 5.1%). Despite this apparent high-quality XRPD characterization, the structure provided still displays large SSNMR errors when shift

(20) (a) Becke, A. D. *J. Chem. Phys.* **1993**, *98*, 5648. (b) Perdew, J. P.; Wang, Y. *Phys. Rev. B* **1992**, *45*, 13244.
(21) Lee, C.; Yang, W.; Parr, R. G. *Phys. Rev. B* **1988**, *37*, 785.
(22) Dewar, M. J. S.; Zoebisch, E. G.; Healy, E. F.; Stewart, J. J. P. *J. Am. Chem. Soc.* **1985**, *107*, 3902.
(23) Leiserowitz, L. *Acta Crystallogr.* **1976**, *B32*, 775.
(24) Li, C.; Johnson, R. P.; Porco, J. A., Jr. *J. Am. Chem. Soc.* **2003**, *125*, 5095

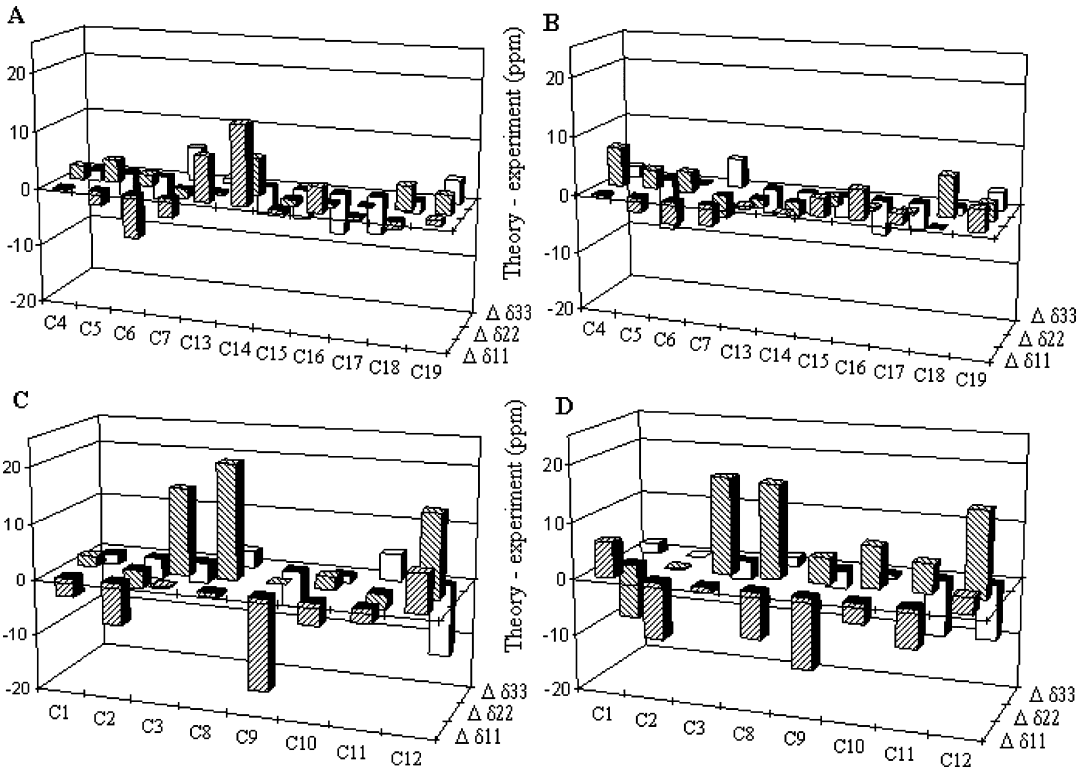


***Figure 5.*** A position-by-position difference plot for the initial SSNMR model (plots A and C) and the final XRPD/SSNMR refined structure (plots B and D). Values plotted are [computed − experimental] principal shift differences (ppm) for all carbons with $sp^3$ carbons shown in the top plots and $sp^2$ positions at the bottom. The $sp^3$ carbons are presently the most sensitive to structure and indicate a poor fit at C14 (plot A), suggesting a structural error within ±2 bonds. In contrast, the errors in $sp^2$ carbons are relatively unchanged by the refinement ($\sigma$ = 8.5 versus 8.3 ppm in plots C and D, respectively) and demonstrate that these carbons are less diagnostic due to systematic errors in the computations used. The final structure shows good fits at all $sp^3$ carbons (plot B), consistent with a correct structure.

tensors computed at the proposed geometry are compared to experimental values. Thus, further refinement that combines the two analyses is suggested.

**Achieving Consistency between NMR and X-ray Data.** Superior refinements should be obtained when both SSNMR and XRPD data are combined, because the two datasets tend to reflect different structural features. Herein, an approach was employed in which the X-ray refined structure was used as input for shift tensor calculations and corresponding errors compared for both data types. Poor fits to either dataset indicate the need for further refinement. SSNMR provides three tensor principal values for each individual atom and thus three fitting parameters, allowing identification of very specific regions of the molecule in need of subsequent refinement. The figures-of-merit used for SSNMR and XRPD data were, respectively, root-mean-squared difference between computed and experimental shifts ($\sigma$) and the weighted Rietveld parameter (wRp). Any necessary refinements were performed using constrained geometry optimization (see Experimental Section) of only the poorly fit segment of the structure with all other regions held constant. A recalculation of errors was then performed to assess the quality of the new structure, and this process repeated until self-consistency was obtained (Figure 2).

In ambuic acid, the initial SSNMR model (**I**, $\sigma$ = 8.3 ppm) allowed for structural solution of the X-ray data using the rigid body assumption, but with a wRp of 14.3%, indicating the need for additional refinement. Simulated annealing was performed with all heavy atom torsion angles allowed to vary over a 360° range to eliminate bias from the initial model and ensure a global optimization. This step provided the structure previously described having a wRp of 5.1% for Rietveld analysis but with an $\sigma$ = 25.1 ppm for SSNMR shift tensors. Prior work has shown that C−H bond length strongly influences NMR fit;[18] thus all C−H bonds were subjected to a DFT optimization at the B3LYP/D95* level. However, this process resulted in little change in either figure-of-merit. Examination of the structure revealed nonoptimal heavy atom bond lengths and valence angles. Refinement of these parameters decreased $\sigma$ to 9.0 ppm while causing little change in the wRp value of roughly 5%. Thus, it appears that a final refinement of bond lengths and valence angles in the best-fit conformation is generally necessary. Despite the improvements, large NMR errors were still observed at atoms in the cyclohexenone ring, suggesting a need to modify the ring structure. Such refinement was performed on all dihedral angles involving at least three ring atoms and decreased $\sigma$ to 7.8 ppm while leaving wRp relatively unchanged. Accurate NMR fitting of the carboxyl group requires that this moiety be paired in a hydrogen-bonding arrangement.[1c] Accordingly, a model was constructed with the carboxyl group bonded to two additional carboxyls in the $2_1$ screw axis specified by the crystal structure. This structure had $\sigma$ = 7.0 ppm and wRp = 4.77%. The final Rietveld fit to the powder pattern is shown in Figure 3. The unit cell parameters previously listed were obtained from this final fit. Final refined coordinates are included as Supporting Information. Figure 4 provides an illustration of error versus step number for the described process.

In the final structure, a comparison of all non-hydrogen dihedral angles from the SSNMR/XRPD analysis with structure **I** shows that the angles differ by greater than 35° at only two positions. Specifically, differences of 36.9° and 103.0° were

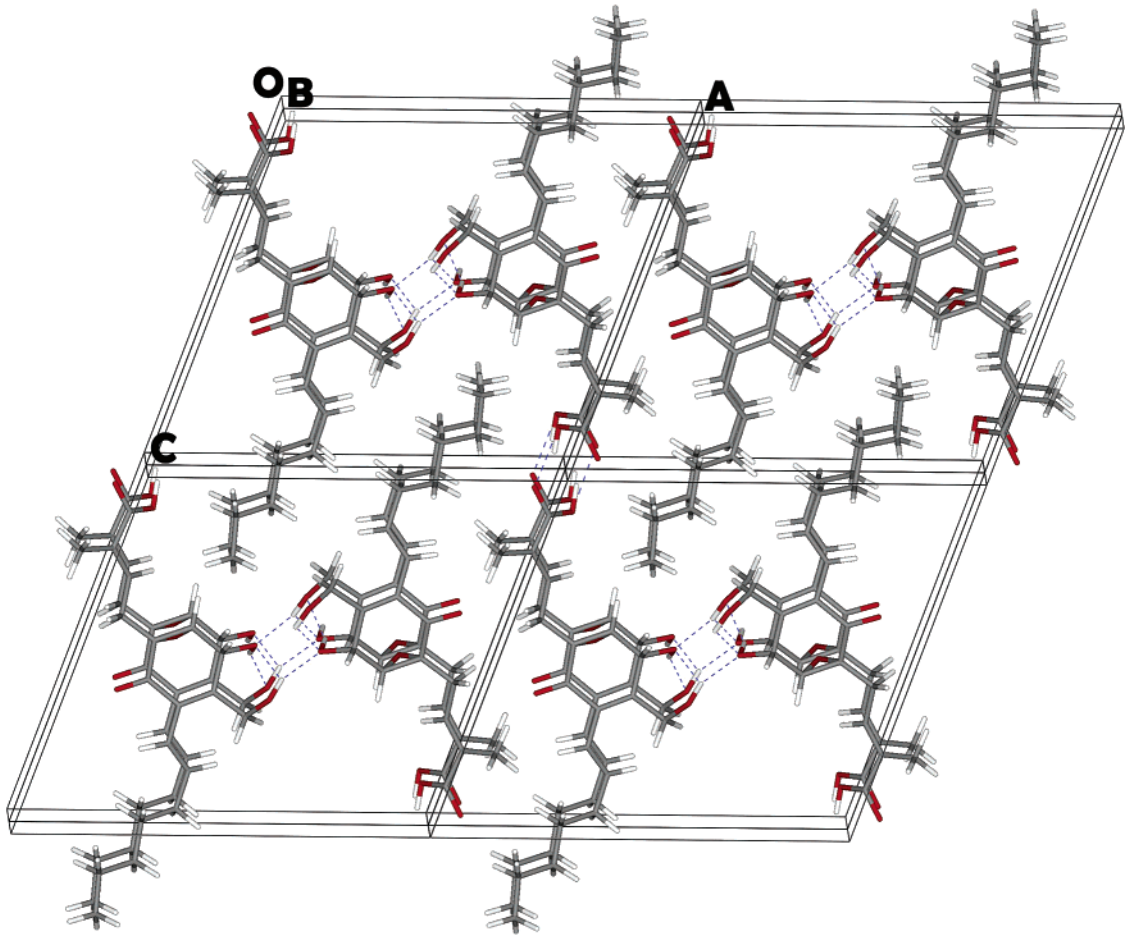


***Figure 6.*** The arrangement of ambuic acid in the unit cell.

found in the C3−C4−C5−C10 and C11−C12−C13−C14 angles, respectively. All other dihedral angles differ by an average of only ±5.5°, generally supporting prior SSNMR predictions of structure. The correction about the C4−C5 bond was not surprising as the predicted SSNMR error in this position was ±44°.[1c] In contrast, modeling of the C12−C17 region was previously omitted to reduce computational costs. However, the prior selection of the gas-phase energy minimum ignores the fact that molecular segments may assume less favorable conformations when lattice forces are present. The XRPD corrects this structural error and emphasizes the synergy between the two techniques. Nevertheless, it should be noted that the experimental SSNMR data, in fact, also reflect such nonbonded interactions. This is true in general because nonbonded interactions cause conformational changes and such rotations are strongly reflected in tensor shifts. Hence, future SSNMR analyses may provide more accurate starting structures, especially when improved data analysis schemes are used.

**Improving the NMR Model.** To obtain more accurate structures from SSNMR data, we examined deviations between experimental NMR tensor shifts and computed values on an atom-by-atom basis for the proposed energy minimized structure. This procedure is preferable to examining a single figure-of-merit for the total structure because it ensures that no outliers are missed when the figure-of-merit is heavily weighted in favor of well-fit data. This approach may be applied to entire structures as shown in Figure 5 where differences in principle values at all positions are plotted with $sp^3$ carbons shown in the top two figures and $sp^2$ in the bottom two. These figures identify significant errors (i.e., $>3\sigma$) in the initial SSNMR model (plots A and C) at positions 3, 8, 9, 12, and 14. The errors at $sp^2$ carbons (i.e., C3, C8, C9, and C12) likely reflect a deficiency of the computational methods in adequately treating electron correlation.[1c,25] In ambuic acid, this shortcoming in theory is anticipated to be especially evident as carbons 8, 9, and 12 are part of a cross conjugated moiety. The influence of cross conjugation on computed shift tensors appears to have been unstudied, but the results here suggest that tensors calculated for such carbons are relatively inaccurate (Figure 5C and D). It is notable that such systems are rigid and planar to allow maximum delocalization of $\pi$-electrons. Thus, accurate conformations are usually predictable, and the poor tensor fits likely reflect computational limitations rather than structural errors. In contrast, the errors at C14, an $sp^3$ carbon, are indicative of a nearby structural error consistent with the X-ray modification of the C11−C12−C13−C14 angle. A structural error will, in general, be within two bonds of a poorly fit carbon. The corrected conformation reduces the errors at carbons 13−17 from 6.4 to 3.8 ppm. This improved fit also resolves a previous ambiguity[1c] in chemical shift assignments at carbons 13, 14, and 15 and reassigns these shifts as summarized in Table 1.

(25) Harper, J. K.; Mulgrew, A. E.; Li, J. Y.; Barich, D. H.; Strobel, G. A.; Grant, D. M. *J. Am. Chem. Soc.* **2001**, *123*, 9837.

***Table 1.*** Revised Chemical Shift Assignments in Ambuic Acid, Experimental (Theoretical)

| position | isotropic | $\delta_{11}$ | $\delta_{22}$ | $\delta_{33}$ |
|---|---|---|---|---|
| C13[a] | 34.0 (35.0) | 47.1 (48.6) | 39.2 (43.5) | 15.8 (13.0) |
| C14 | 26.8 (27.5) | 36.5 (39.3) | 30.2 (31.5) | 13.8 (11.6) |
| C15[a] | 35.2 (33.9) | 52.4 (53.5) | 39.8 (39.5) | 13.5 (8.6) |

[a] Shift assignments are reversed relative to original ordering. Shift assignment at C14 remains unchanged, but is now given at high statistical probability of >90%.

***Table 2.*** Hydrogen-Bonding Geometry (Å, deg)

| D–H···A | D–H | H···A | D···A | D–H···A |
|---|---|---|---|---|
| O19−H···O7 | 0.965 | 2.317 | 2.969 | 124.25 |
| O19−H···O7 | 0.965 | 1.974 | 2.714 | 131.79 |
| O7−H···O19 | 0.966 | 2.006 | 2.814 | 139.85 |

NMR errors in the final structure are shown in Figure 5B for $sp^3$ carbons with all positions now accurately fit.

**Evaluating Hydrogen Bonding.** The final XRPD refinement provides lattice detail for non-hydrogen atoms, but hydrogen positions remain essentially unknown. In the case of hydroxyl hydrogens, structural characterization is improved by additional refinement. In ambuic acid, a model was thus constructed that included all intermolecular hydrogen-bonding partners, with non-hydrogen atoms placed in X-ray refined positions. A constrained semiempirical optimization of H's in O−H···O bonds was then performed (see Experimental Section) in which only hydrogen positions were allowed to vary. Optimized H−O−C7−C8 and H−O−C19−C8 angles of −61.6° and 71.4° were observed, respectively, versus corresponding values of −71.6° and 67.6° from the original NMR data. These dihedral angles refer to Newman projections that place the H at the front and define clockwise rotations as positive from a 0° position having the H−O and the C−C bonds eclipsed. NMR shift calculations on gas-phase molecules are thus able to characterize lattice conformations when combined with experimental data. The accuracy of the NMR angles probably reflects the fact that $^{13}C$ tensors in C−OH moieties are determined primarily by the position of the oxygen lone pairs and to a much lesser extent by the presence or absence of hydrogen bonding.[18,26] The final hydrogen-bonding arrangement and lattice structure is shown in Figure 6 and involves three distinct O−H···O interactions (Table 2).

## Conclusions

Structural characterizations in microcrystalline materials are improved by combining X-ray powder and solid-state NMR data. The methods proposed here are particularly suited to organic materials because these contain nuclei readily examined by NMR but which diffract weakly in typical X-ray powder analysis. The advantages of this approach result from the ability of NMR to provide high-quality local structural detail including hydrogen positions and the sensitivity of X-ray analysis to intermolecular interactions and lattice order. In ambuic acid, these combined methods provide the first verification and refinement of a structure proposed primarily from SSNMR data.

**Acknowledgment.** Computer support for all geometry optimizations and NMR tensor calculations was provided by the Center for High Performance Computing at the University of Utah. Support for this research was provided by the National Institutes of Health under Grant No. 5R01GM08521-42 to D.M.G. Work at the Advanced Photon Source was supported by the U.S. Department of Energy, Office of Science, Office of Basic Energy Sciences, under contract W-31-109-Eng-38. We thank Professor Gary Strobel for helpful discussions regarding the ubiquitous occurrence of ambuic acid.

**Supporting Information Available:** Refined coordinates for ambuic acid, structure **I**, and complete refs 10 and 19. This material is available free of charge via the Internet at http://pubs.acs.org.

JA055570J

(26) (a) Harper, J. K.; Grant, D. M. *J. Am. Chem. Soc.* **2000**, *122*, 3708. (b) Liu, F.; Orendt, A. M.; Alderman, D. W.; Grant, D. M. *J. Am. Chem. Soc.* **1997**, *119*, 8981. (c) Liu, F.; Phung, C. G.; Alderman, D. W.; Grant, D. M. *J. Magn. Reson., Ser. A* **1996**, *1120*, 242.